Flow-Regulated Growth of TiO2 Nanotubes in Microfluidics

Rong Fan, Xinye Chen, Zihao Wang, David Custer, Jiandi Wan. Rochester Institute of Technology, Rochester, NY. Email: jdween@rit.edu.

Due to the functioanl material properties of TiO2 and unique geometric features of nanotubes, TiO2 nanotubes find applications in a wide range of fields including photocatalysis, solar cells, electrochromic devices, sensors, biocoating, and drug delivery. Self-organized TiO2 nanotube arrays are commonly produced via electrochemical anodization of Ti in a fluoride-containing electrolyte solution and a complex field-aided oxidation and dissolution process is responsible for the formation of TiO2 nanotubes. To date, all electrochemical anodization approaches are conducted in bulk conditions (e.g., the distance between the anode and cathode is in the range of centimeter) and long anodization time is required to obtain high aspect ratio TiO2 nanotubes, which normally leads to inhomogeneous tube diameters and structures. Although introducing hydrodynamic factors such as stirring to the electrolyte solution during anodization has shown to be able to improve the formation of TiO2 nanotubes, quantitative and mechanistic investigation of the growth of TiO2 nanotubes in well-controlled flow conditions is missing. Here, we developed a microfluidic approach to grow TiO2 nanotubes directly inside the microfluidic channel using electrochemical anodization and showed that, without the change of applied voltage and the composition of electrolytes, flow alone can significantly enhance the growth of TiO2 nanotubes and control the tube structures. In addition, by adjusting the velocity profile of the flow inside microfluidic channel, the spatial distribution of TiO2 nanotubes can be controlled accordingly. By patterning Ti on silicon surfaces in a microfludic channel, we further showed that TiO2 nanotubes can grow in areas with arbitrary shapes. Strikingly, horizontal growth of TiO2 nanotubes was also observed on silicon substrate, opening a new door to spatially manipulate the growth of TiO2 nanotubes and construct hierarchical TiO2 nanotube arrays. Our results thus demonstrate previously unidentified regulatory roles of flow in the growth of TiO2 nanotubes and will impact broadly on the research of TiO2 nanotubes and related applications. *Small,* 2017, 13, 1701154. Patent pending.

I. Microfluidic setup

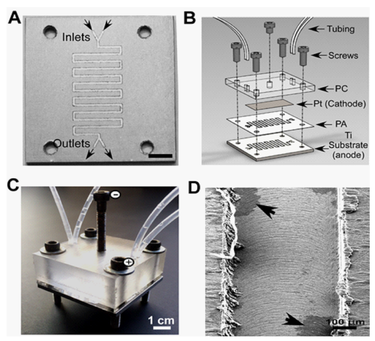

Figure 1. Schematics of the microfluidic setup for fabrication of TiO2 nanotubes. (**A**) Microfluidic channel fabricated on titanium by micromachining (scale bar = 2 cm). Arrows indicate the direction of flow. (**B**) Schematic of the assembly of the microfluidic device. PC: polycarbonate; PA: polyacrylate. (**C**) A bright-field image of the assembled microfluidic device. (**D**) SEM image of TiO2 nanotube-covered microfluidic channel. Arrows indicate the area in the absence of TiO2 nanotubes.

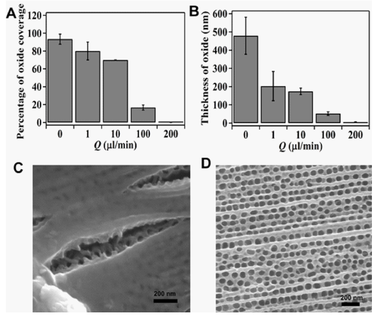

Figure 2. Effect of flow rate on the growth of oxide layer at the oxide-electrolyte interface. (**A**) Percentage of the oxide coverage at different flow rates in the microfluidic channel. (**B**) The change of thickness of the oxide layer with flow rates. (**C**) & (**D**) SEM images of the oxide layer at the flow rate of 1 µl/min and 200 µl/min, respectively.

II. Effect of flow rate on the growth of TiO2 nanotube arrays in microfluidics

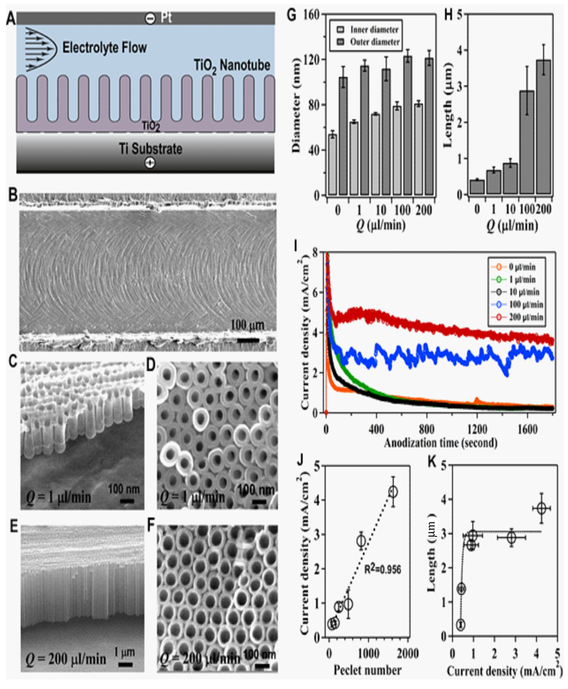

Figure 3. Effect of flow rate on the growth of TiO2 nanotubes in microfluidics. (**A**) Schematic of the generation of TiO2 nanotubes via electrochemical anodization under flow conditions in a microfluidic channel. (**B**) Rrepsentative SEM image of a TiO2 nanotube-covered microfluidic channel. (**C**) & (**D**) SEM images of side view and top view, respectively, of TiO2 nanotubes fabricated at a flow rate of 1 µl/min. (**E**) & (**F**) SEM images of side view and top view, respectively, of TiO2 nanotubes fabricated at a flow rate of 200 µl/min. (**G**) Effect of flow rate on the inner and outer diameters of TiO2 nanotubes. (**H**) Effect of flow rate on the length of TiO2 nanotubes. (**I**) Effect of flow rate on the change of current density during anodization. (**J**) Dependence of the equillibrium current density on Peclet number (Pe = Lv/D, where L is the width of the channel, v is the velocity of the fluid, and D is the diffusion coeffient). Dot line is a linear regression fitting curve with a correlation coefficient of 0.956. (**K**) Dependence of the length of TiO2 nanotubes on the equillibrium current density.

III. Control the spatial growth of TiO2 nanotubes in microfluidics

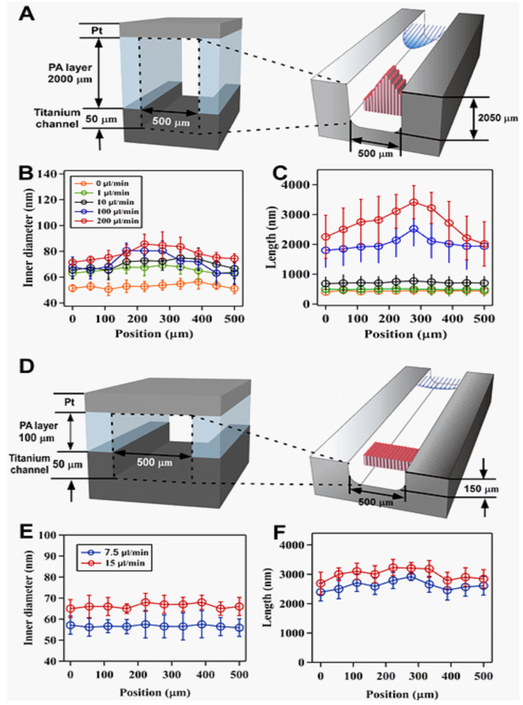

Figure 4. Control the spatial growth of TiO2 nanotubes in microfluidics. (**A**) Schematics of the cross-sectional view of a microluidic channel with a width of 500 µm and a height of 2050 µm. Note that because the height of the channel is much larger than the width of the channel, the flow in the channel is expected to be parabolic in the x-y plane. (**B**) & (**C**) The change of inner diameter and length of TiO2 nanotubes, respectively, across the width of a channel fabricated at different flow rates in a microfluidic device shown in (A). (**D**) Schematics of the cross-sectional view of a microluidic channel with a width of 500 µm and a height of 150 µm. In this case, the height of the channel is smaller than the width of the channel, the flow streamline in the channel is expected to be flat in the x-y plane but parabolic in the x-z plane. (**E**) & (**F**) The change of inner diameter and length of TiO2 nanotubes, respectively, across the width of a channel fabricated at flow rates of 7.5 and 15 µl/min in a microfluidic device shown in (D). Note that flow rates of 7.5 and 15 µl/min in device (D) give the same velocity (or Peclect number) in device (A) when flow rates of 100 and 200 µl/min are used, respectively.

IV. Patterning and horizontal growth of TiO2 nanotubes on silicon

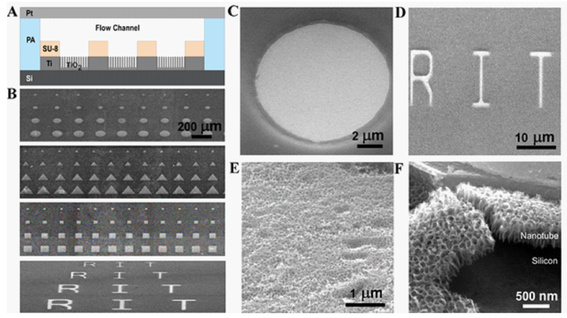

Figure 5. Patterning TiO2 nanotubes on silicon substrates. (**A**) Schematic of patterning TiO2 nanotubes on silicon in a microfluidic channel. (**B**) SEM images of patterned TiO2 nanotubes on silicon. (**C**) & (**D**) High resolution SEM images of TiO2 nanotubes patterned in a circular shape and the letters of "RIT" respectively. (**E**) & (**F**) High resolution SEM images of the top view and side view TiO2 nanotubes, respectively, inside the circular pattern shown in C.

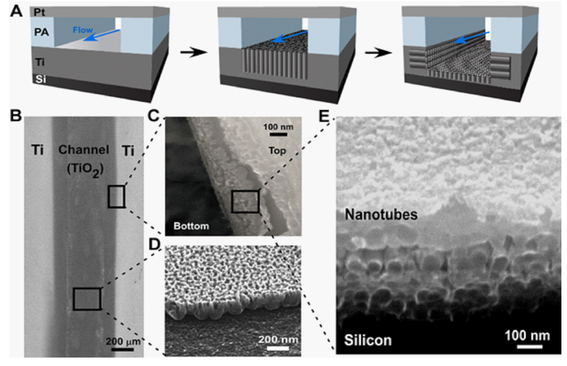

Figure 6. Horizontal growth of TiO2 nanotubes on silicon. (**A**) Schematics of the growth of TiO2 nanotubes on silicon in a microfluidic channel. (**B**) Representative SEM image of Ti on silicon substrate after anodization in a microfluidic channel. (**C**) SEM image of the edge of microfluidic channel where Ti was anodized to produce TiO2 nanotubes. Bottom: silicon; top: Ti. (**D**) High resolution SEM image of TiO2 nanotubes growing in the horizontal direction in the side wall of the channel. (**E**) SEM image of TiO2 nanotubes growing in the center of the microfluidic channel.